Supernova remnants as sources of cosmic rays and nonthermal emission

V.N.Zirakashvili, V.S.Ptuskin

Pushkov Institute of Terrestrial Magnetism, Ionosphere and Radiowave Propagation, Russian Academy of Sciences (IZMIRAN), 108840 Troitsk, Moscow, Russia

Outline

- Diffusive shock acceleration (DSA) of particles in SNRs
- Amplification of magnetic fields in young SNRs
- Modeling of DSA in young and old SNRs
- DSA in wind blown bubbles

Diffusive Shock Acceleration

Krymsky 1977; Bell 1978; Axford et al.1977; Blandford & Ostriker 1978

Very attractive feature: power-law spectrum of particles accelerated, $\gamma=(\sigma+2)/(\sigma-1)$, where σ is the shock compression ratio, for strong shocks $\sigma=4$ and $\gamma=2$

Maximum energy for SN: $D\sim 0.1 u_{sh} R_{sh}$

$\sim 3\cdot 10^{27}$ cm^2/s$<D_{gal}$

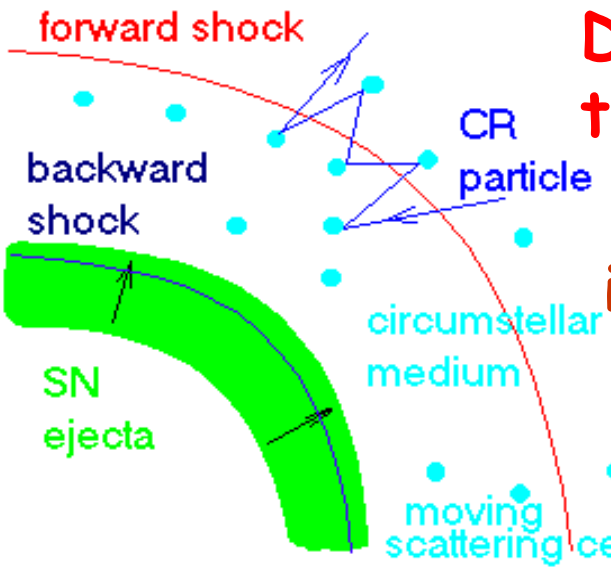

Diffusion coefficient should be small in the vicinity of SN shock

In the Bohm limit $D=D_B=cr_g/3$ and for interstellar magnetic field

$$E_{\max} = Z\cdot 10^{14}\,\mathrm{eV}\left(\frac{B}{10\,\mu\mathrm{G}}\right)\left(\frac{R_{\mathrm{sh}}}{3\,\mathrm{pc}}\right)\left(\frac{u_{\mathrm{sh}}}{3000\,\mathrm{km\,s^{-1}}}\right)$$

X-ray image of Tycho SNR (from Warren et al. 2005)

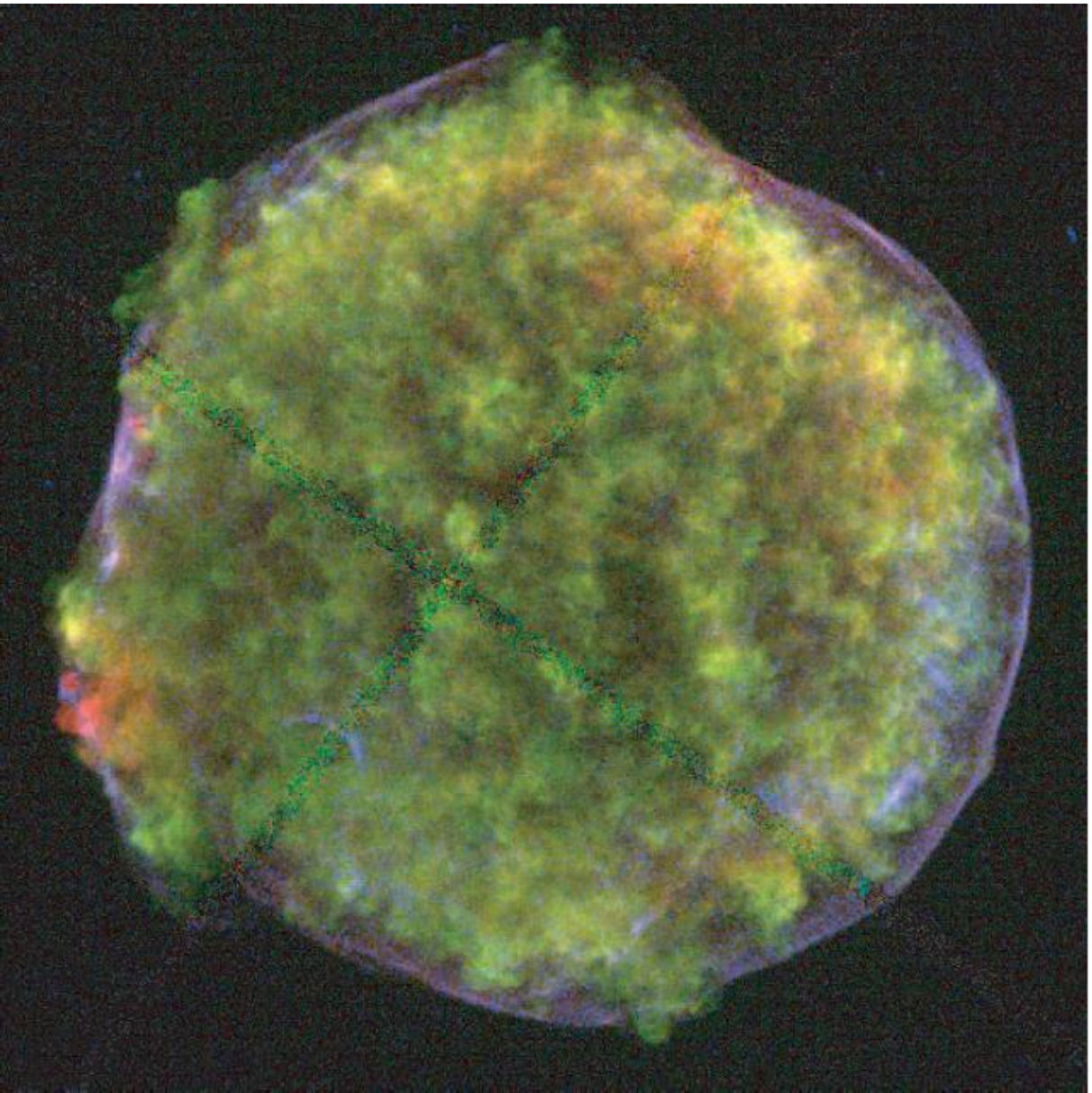

Thin non-thermal X-ray filaments at the periphery of the remnant – evidence of electron acceleration and of magnetic amplification.

Magnetic field amplification by non-resonant streaming instability

Bell (2004) used Achterberg's results (1983) and found the regime of instability that was overlooked

$$F_{CR} = -\frac{1}{c}\left[j_d \times B \right]$$

$$\omega^2 = V_a^2 k^2 - j_d \frac{B_0 k}{c\rho_0}$$

$$k\, r_g >> 1,\ \gamma_{max} = j_d B_0 / 2c\rho V_a$$

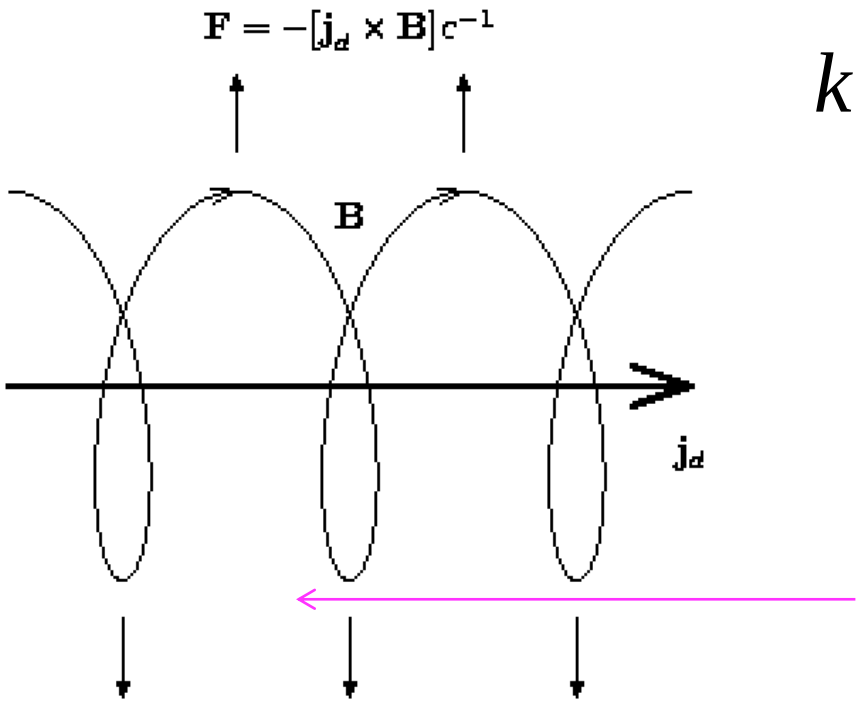

Since the CR trajectories are weakly influenced by the small-scale field, the use of the mean j_d is well justified

E= - [**u**X**B**]/c Regular electric field

Modeling of Bell's instability (Matthews et al. 2017)

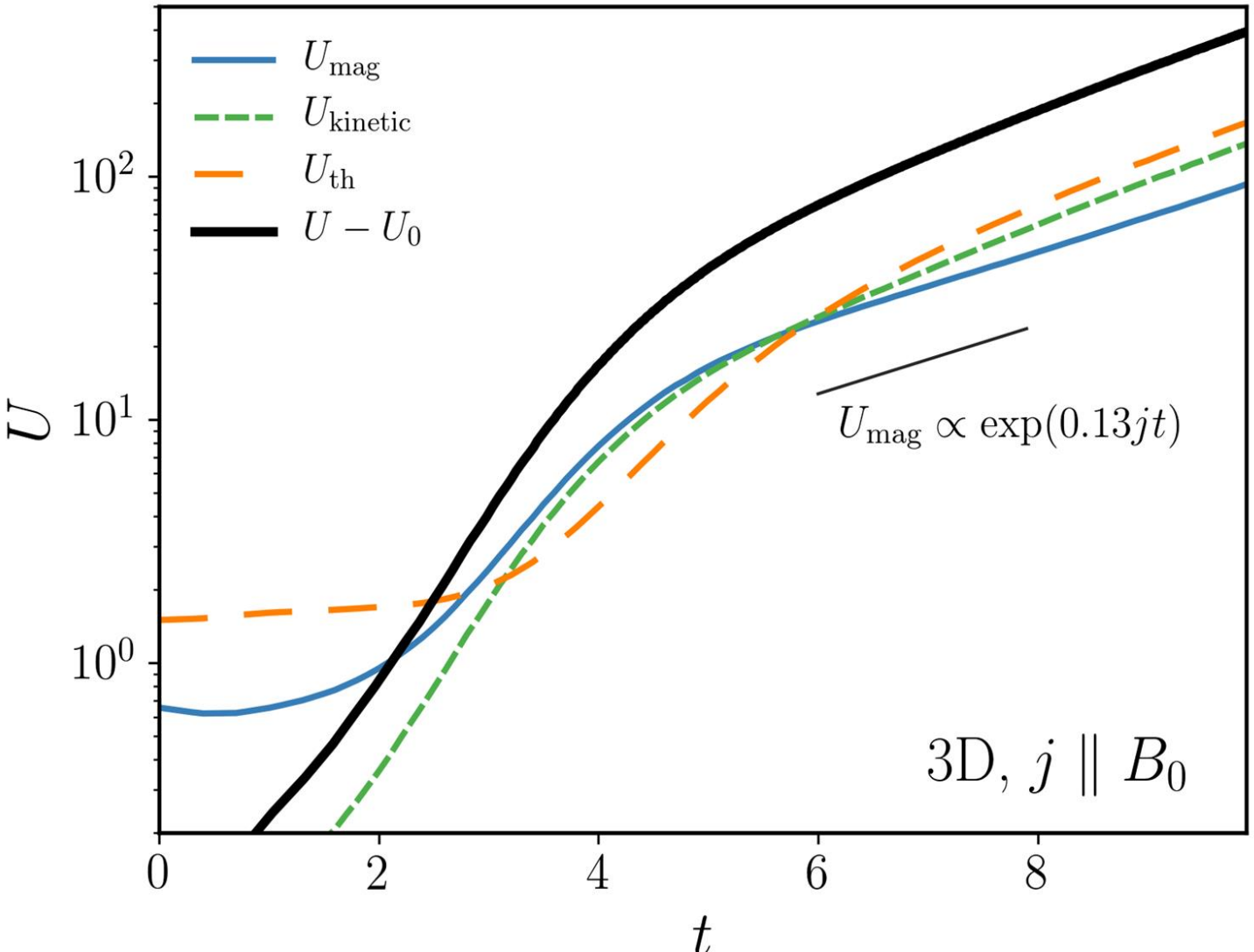

Exponential nonlinear growth (Beresnyak & Li 2014) was confirmed.

•This is important for small initial B_0 e.g. at reverse shocks in SNRs

MHD modeling in the shock transition region and downstream of the shock

Zirakashvili & Ptuskin 2008

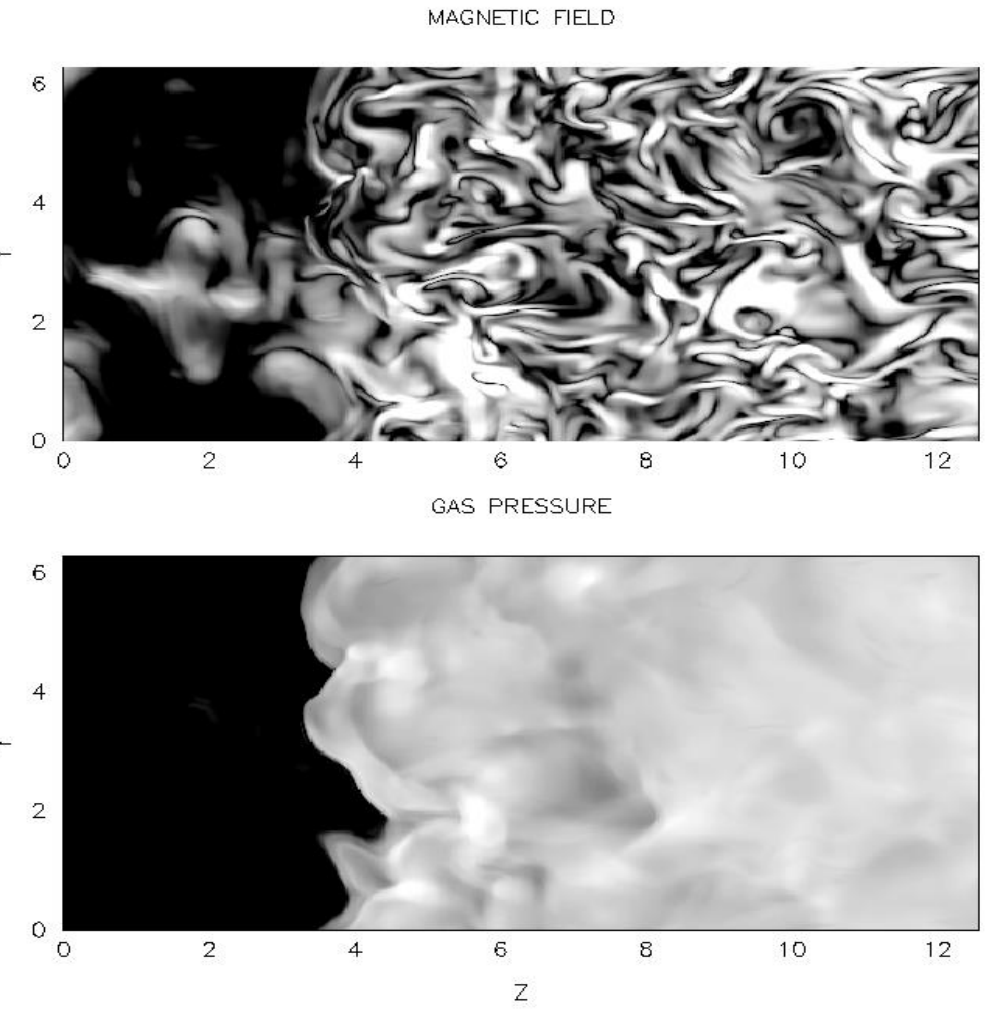

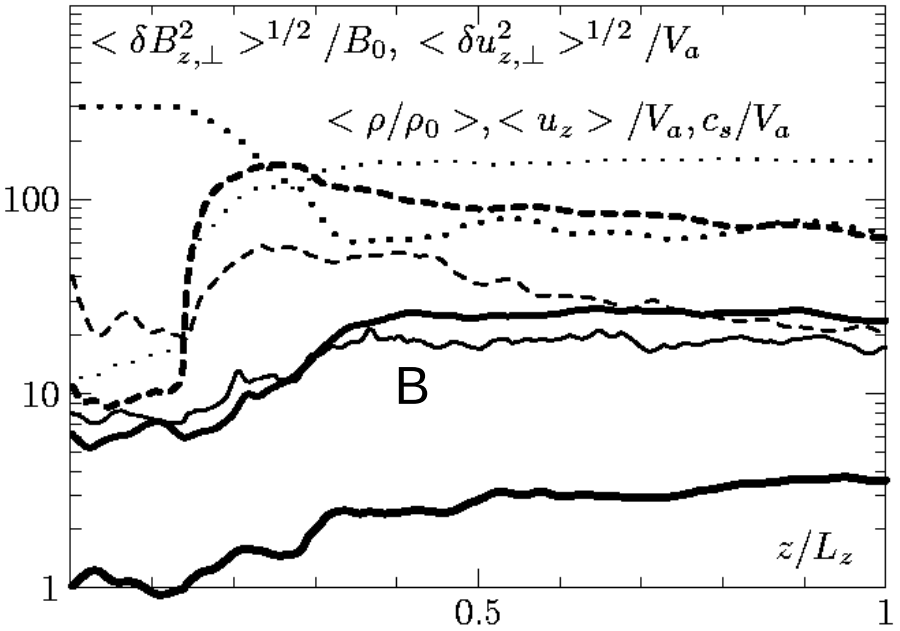

u_1=3000 km/s V_a=10 km/s

η_{esc}=0.14

0.02L

Magnetic field is not damped and is perpendicular to the shock front downstream of the shock!

Ratio=1.4 σ_B=3

3D $256^2 \times 512$

Wood & Mufson 1992

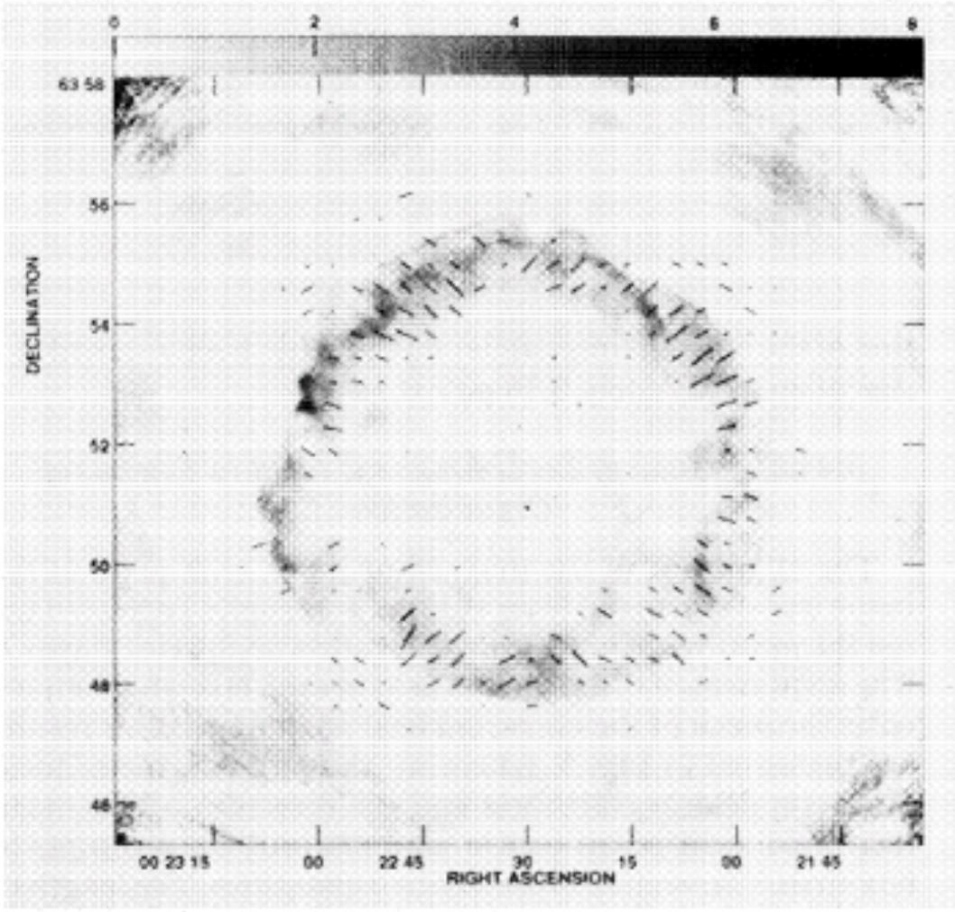

FIG. 5. Map of the remnant of Tycho's supernova showing local magnetic field organization and the direction of the mean local field averaged over boxes of various sizes, superposed on total intensity grey scale as shown in Dickel *et al.* 1991 (Paper I). The length of the vectors indicates the degree of organization in a box, and is proportional to Υ_{org}. The angle of the vector corresponds to the alignment of the mean magnetic field in a box. Positive values of the total intensity are represented with a peak of 8.1×10^{-3} Jy beam^{-1}; the grey scale is in units of 10^{-3} Jy beam^{-1}. (a) Box size of 30×30 pixels (0.55 pc$\times$0.55 pc). (b) Box size of 15×15 pixels (0.27 pc$\times$0.27 pc).

Dickel et al. 1991

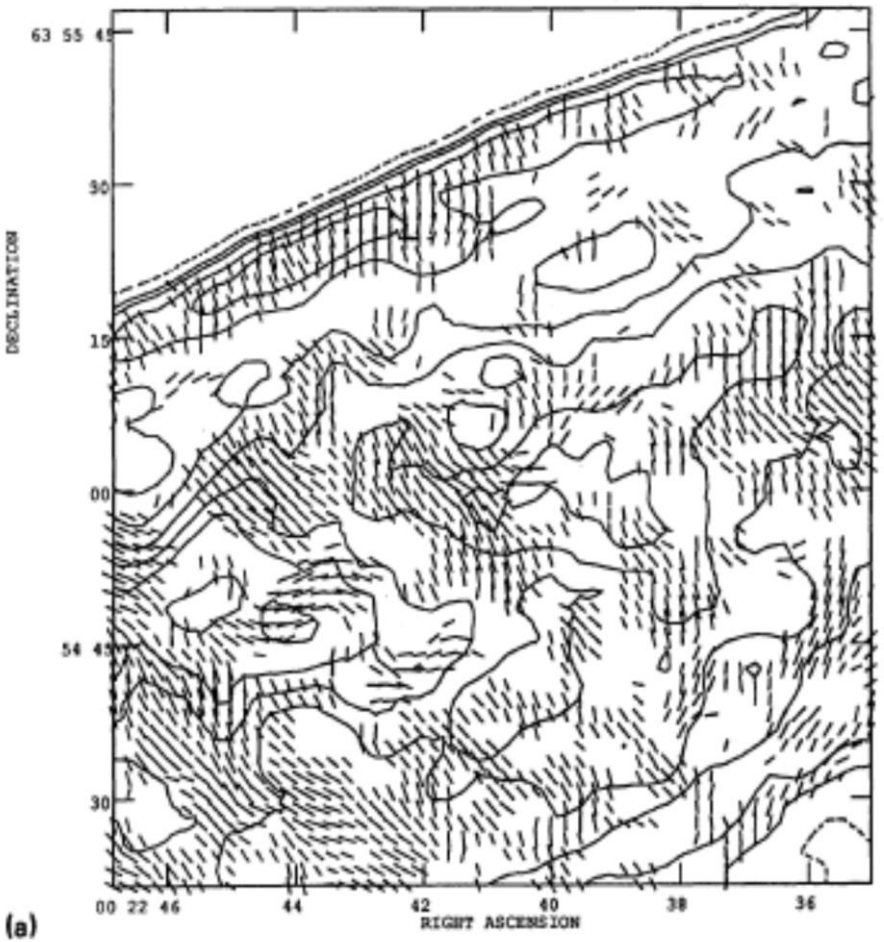

Radial magnetic fields were indeed observed in young SNRs

TeV gamma-rays from young SNRs

Aharonian et al 2008 (HESS)

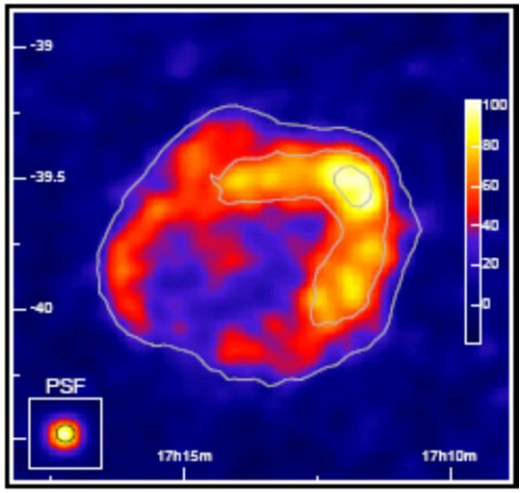

Particles accelerated up to100 TeV in these SNRs. Gamma-rays can be produced in pp collisions (hadronic models) or via the Inverse Compton scattering of IR and MWBR photons on the electrons accelerated (leptonic models)

Aharonian et al 2007 (HESS)

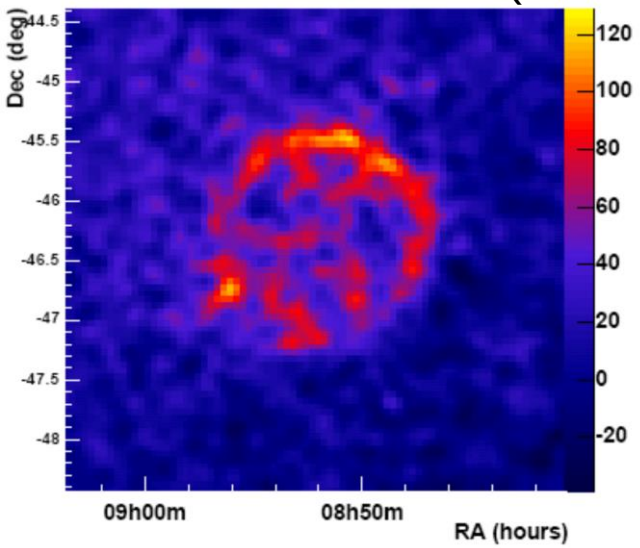

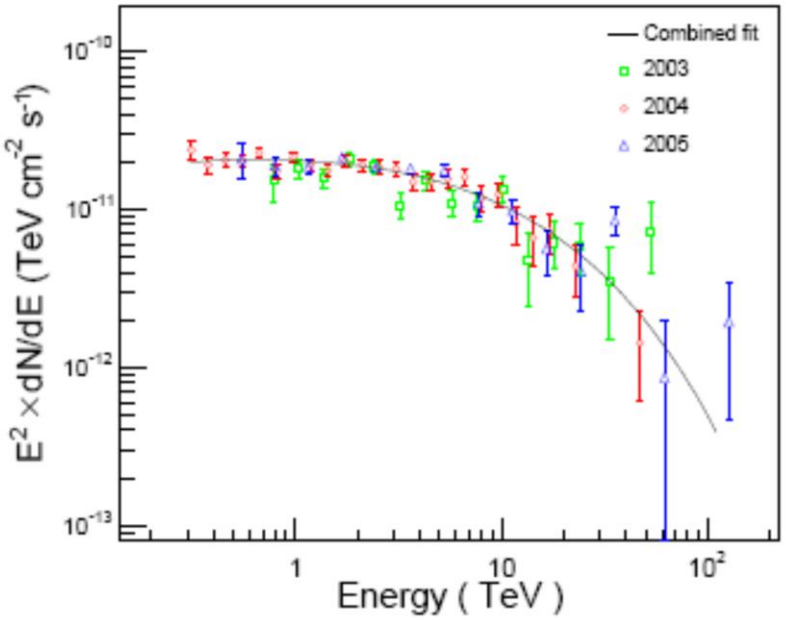

RX J1713.7-3946

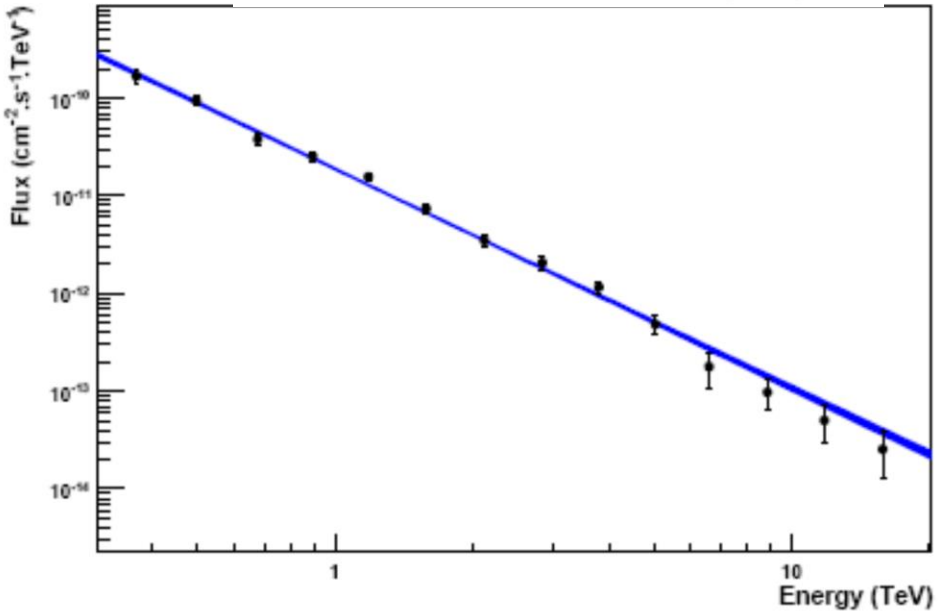

Vela Jr

Old SNRs (T>10^4 yr) in the dense medium

(Ackermann et al. 2013)

$n_H > 1\ cm^{-3}$

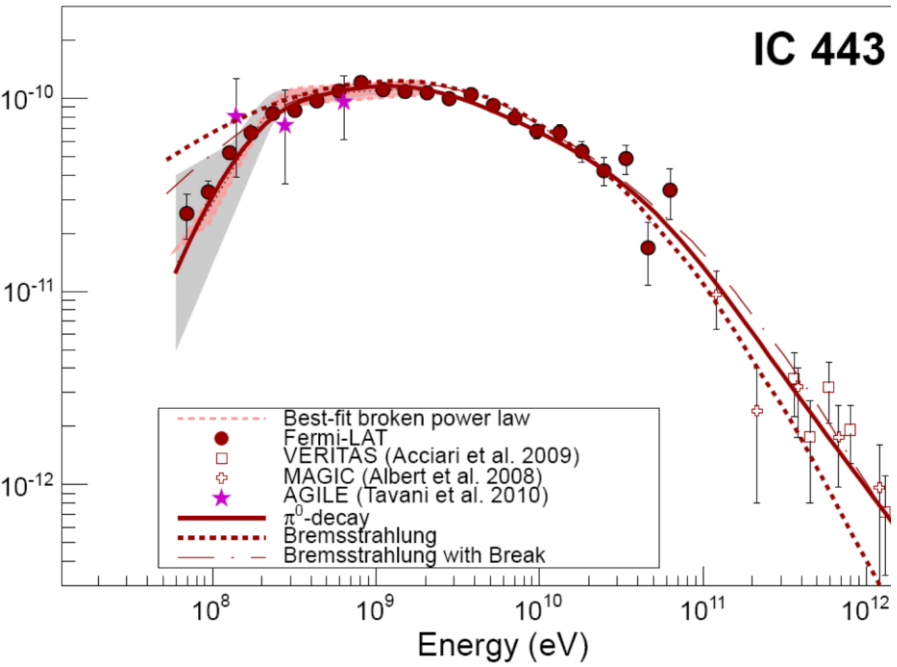

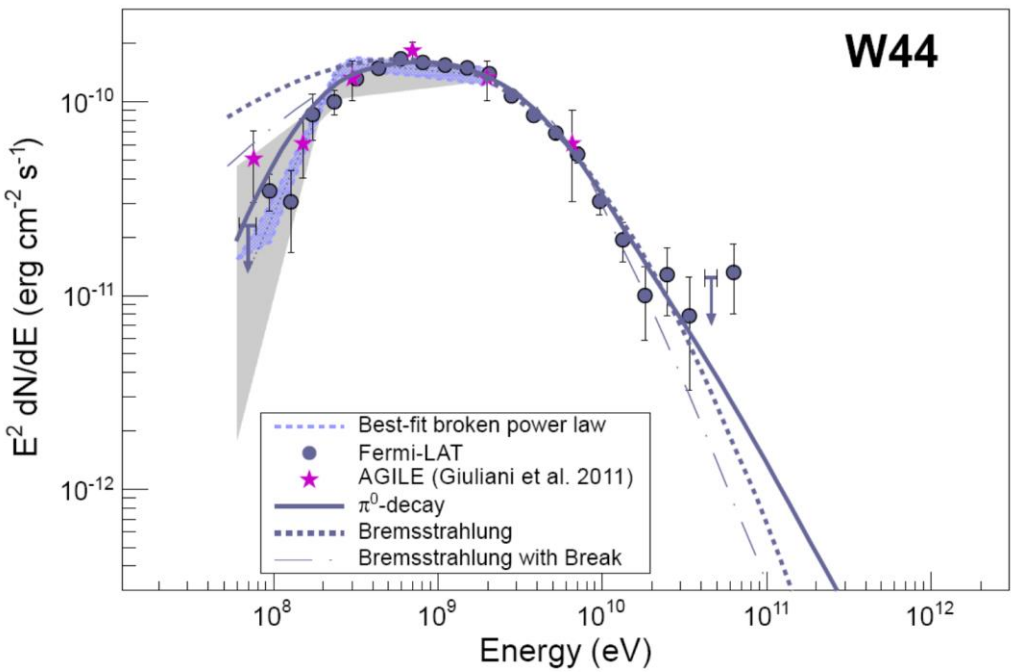

Old SNRs show gamma-ray spectra with steeper parts or cut-offs. TeV protons are not accelerated at present.

E_{max} ~100 GeV in IC443 and E_{max} ~10 GeV in W44. Probably because of neutral damping of MHD waves generated by accelerated particles.

The spectral shape at E<1 GeV favors a hadronic origin of gamma-emission.

Numerical model of nonlinear diffusive shock acceleration

(Zirakashvili & Ptuskin 2012)

(natural development of existing models of Berezhko et al. (1994-2006), Kang & Jones 2006, see also half-analytical models of Blasi et al.(2005); Ellison et al. (2010))

$$\frac{\partial \rho}{\partial t} = -\frac{1}{r^2}\frac{\partial}{\partial r} r^2 u \rho \qquad (1)$$

$$\frac{\partial u}{\partial t} = -u\frac{\partial u}{\partial r} - \frac{1}{\rho}\left(\frac{\partial P_g}{\partial r} + \frac{\partial P_c}{\partial r}\right) \qquad (2)$$

$$\frac{\partial P_g}{\partial t} = -u\frac{\partial P_g}{\partial r} - \frac{\gamma_g P_g}{r^2}\frac{\partial r^2 u}{\partial r} - (\gamma_g - 1)(w-u)\frac{\partial P_c}{\partial r} \qquad (3)$$

$$\frac{\partial N}{\partial t} = \frac{1}{r^2}\frac{\partial}{\partial r} r^2 D(p,r,t)\frac{\partial N}{\partial r} - w\frac{\partial N}{\partial r} + \frac{\partial N}{\partial p}\frac{p}{3r^2}\frac{\partial r^2 w}{\partial r}$$

$$+\frac{\eta_f \delta(p-p_f)}{4\pi p_f^2 m}\rho(R_f+0,t)(\dot{R}_f - u(R+0,t))\delta(r-R_f(t))$$

$$+\frac{\eta_b \delta(p-p_b)}{4\pi p_b^2 m}\rho(R_b-0,t)(u(R_b-0,t)-\dot{R}_b)\delta(r-R_b(t)) \qquad (4)$$

Spherically symmetric HD equations + CR transport equation

Acceleration at forward and reverse shocks

Radio-image of Cas A

Atoyan et al. 2000

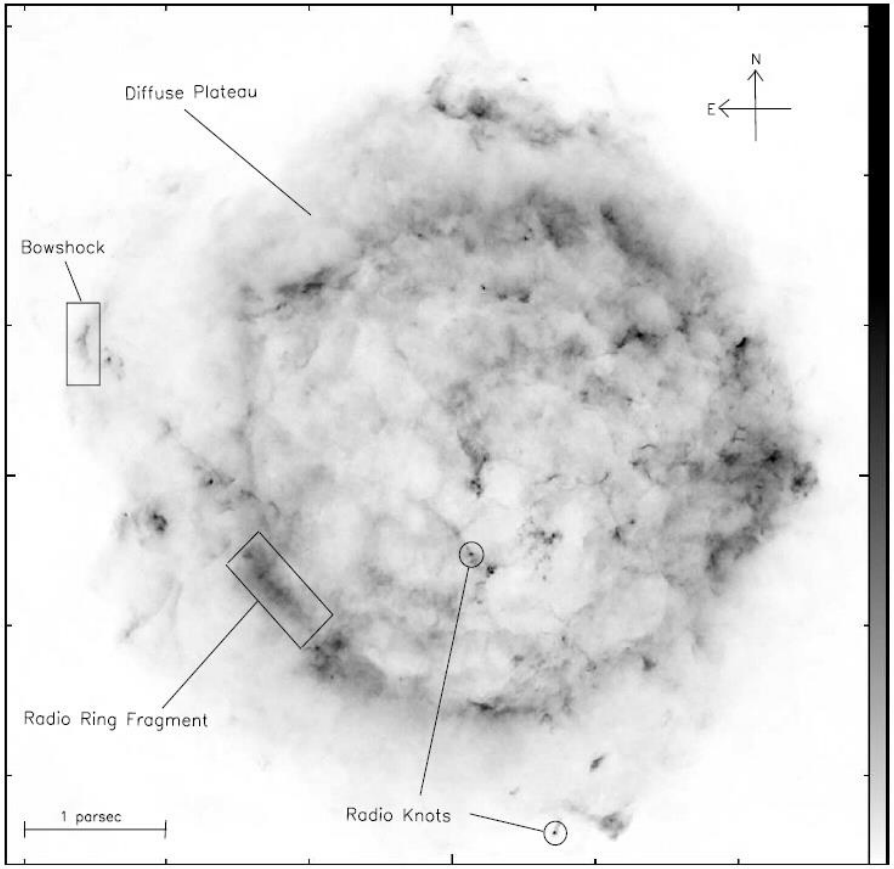

X-ray image of Cas A (Chandra)

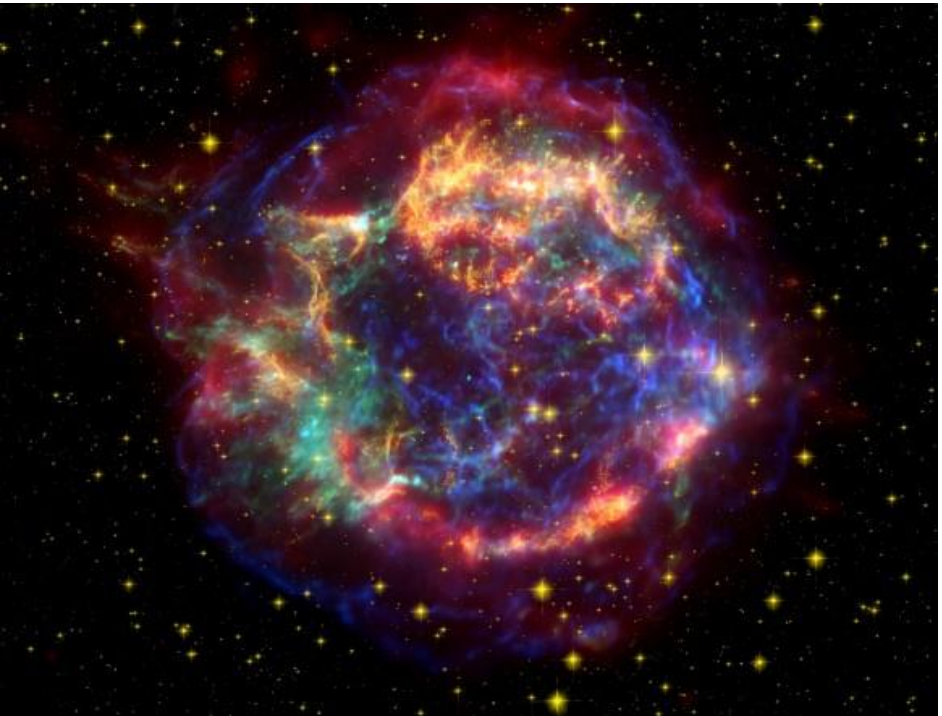

Inner bright radio- and X-ray-ring is related with the reverse shock of Cas A while the diffuse radio-plateau and thin outer X-ray filaments are produced by electrons accelerated at the forward shock.

Fermi gamma ray image of W28 (Hanabata et al. 2014)

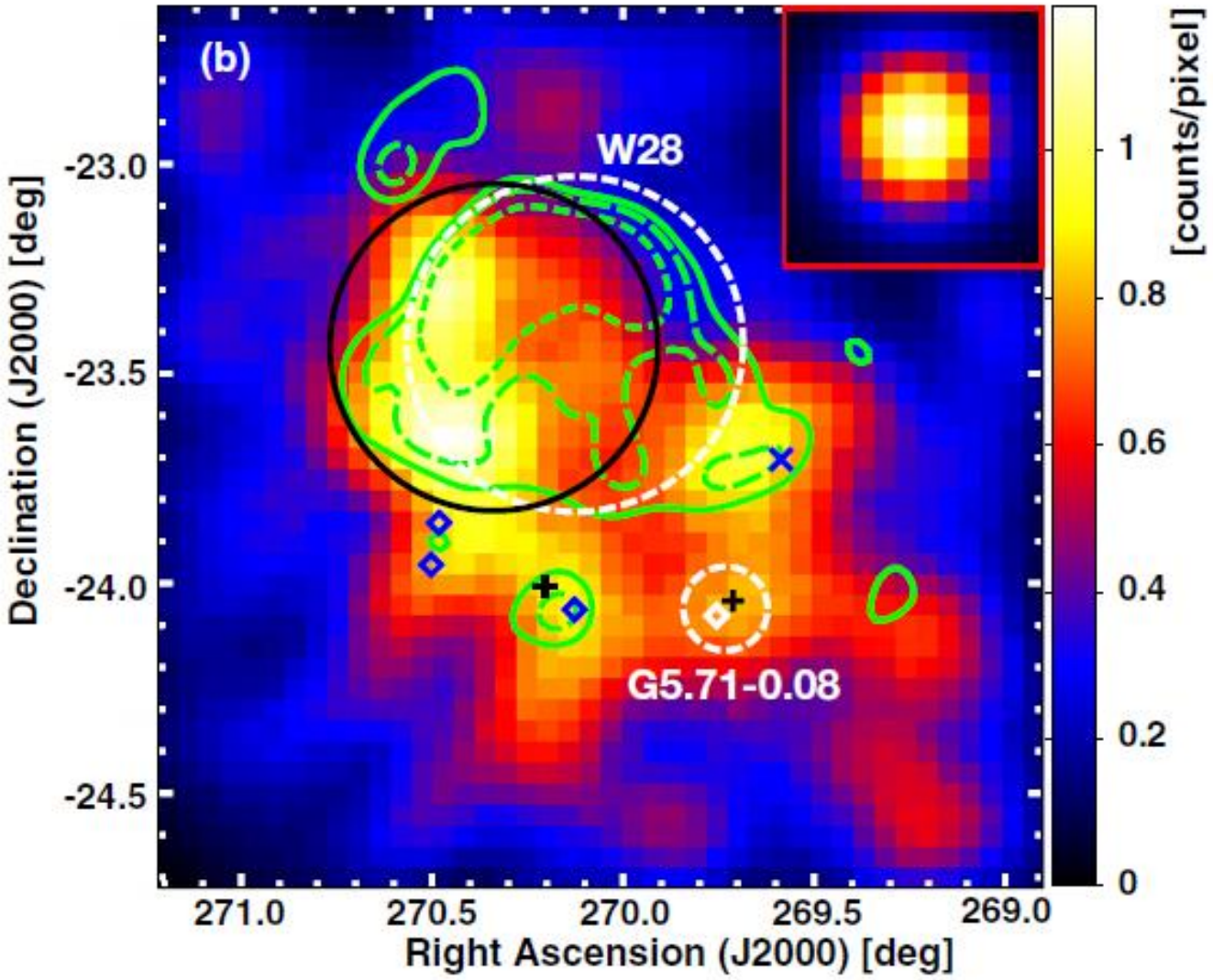

T

Modeling of DSA in young SNR Cas A (Zirakashvili et al 2014) and old SNR W28 (Zirakashvili & Ptuskin 2017)

TABLE I. Physical parameters of SNRs W28 and Cas A

	d	R_f	E_{SN}	M_{ej}	n_H	n_n	K_{ep}	T	V_f	B_f
	kpc	pc	10^{51}erg	$M_\odot$	cm^{-3}	cm^{-3}		kyr	km/s	μG
W28	1.9	13.4	1.3	6.8	4.0	0.2	0.008	37	121	79
Cas A	3.4	2.5	1.2	2.0	0.4	0.0	$4 \cdot 10^{-4}$	0.33	5800	1100

Spectra of particles at FS and RS

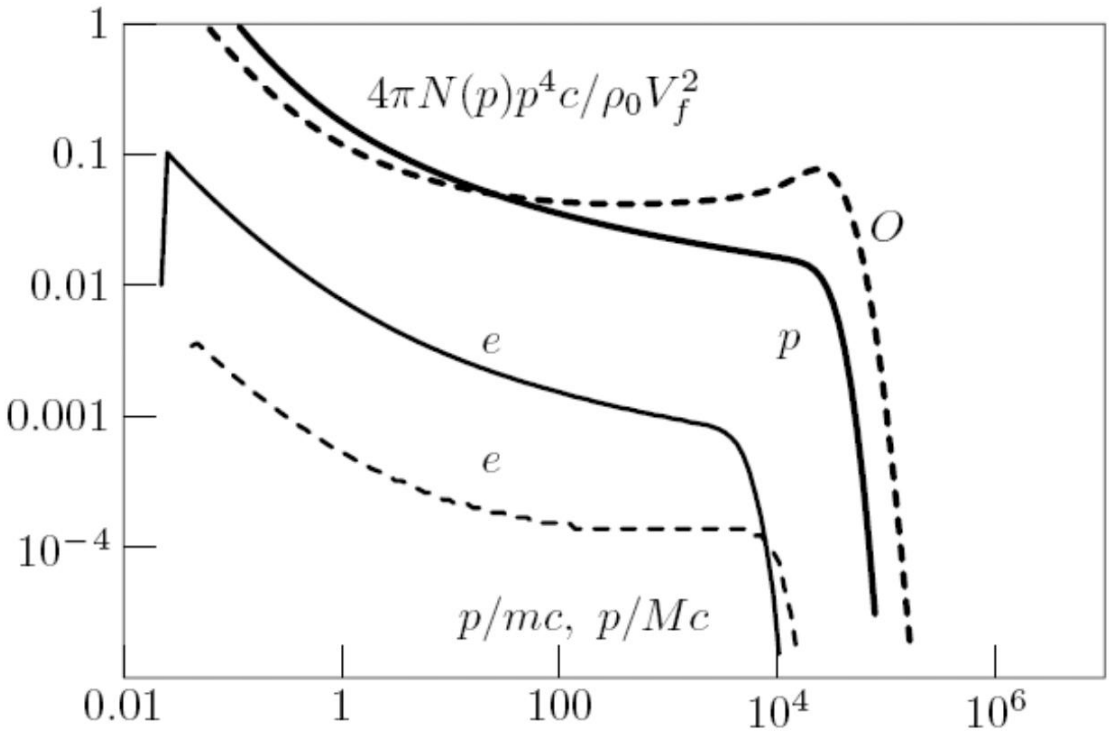

Fig. 3.— The energy distributions of protons at the forward shock (thick line), of oxygen ions at reverse shock (thick dashed line), of electrons at the forward shock (multiplied to the factor of 10^2, thin lines) and of electrons at the reverse shock (thin dashed line) calculated for the model H1 at the epoch $t = 330$ yr. Particle momenta are normalized to the proton mass m and the mass of oxygen ion M. The oxygen spectrum is normalized to the nucleon number density.

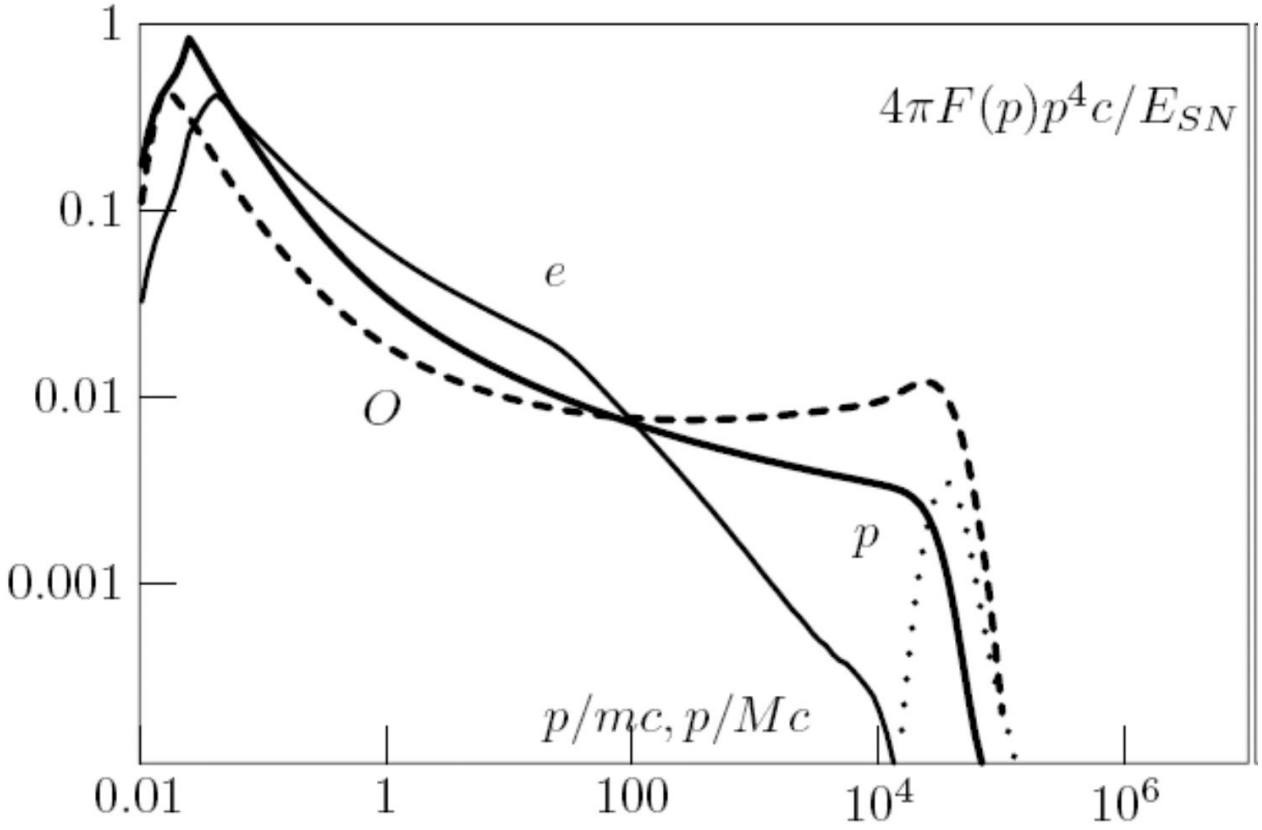

Fig. 4.— Spatially integrated spectra of accelerated protons (solid line), oxygen ions (dashed line) and electrons multiplied to 10^3 (thin solid line) at $t = 330$ yr obtained in the model H1. Spectrum of run-away protons which have left the remnant is also shown (dotted line).

Volume-integrated spectra

E_{max}=80 TeV in hadronic model H1

Spectra of electromagnetic radiation of Cas A

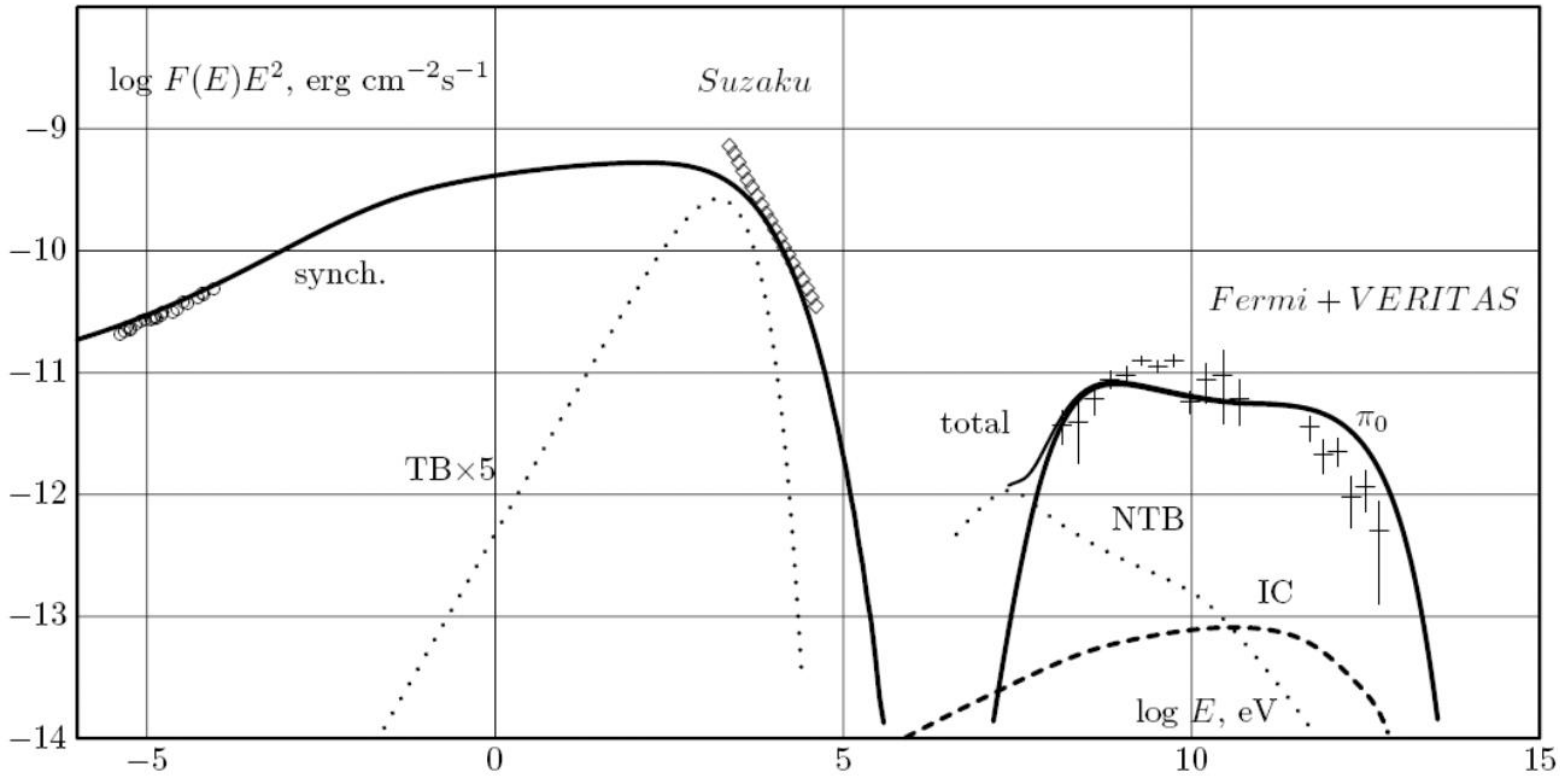

RS dominates in X-rays and gives a significant contribution in gamma-rays and radio

Fig. 6.— The broad-band spectral energy distribution of nonthermal radiation of Cas A calculated within the hadronic model H1. The following radiation processes are taken into account: synchrotron radiation of accelerated electrons (solid curve on the left), IC emission (dashed line), gamma-ray emission from pion decay (solid line on the right), thermal bremsstrahlung (dotted line on the left), nonthermal bremsstrahlung (dotted line on the right). Experimental data in gamma-ray (Fermi LAT, present work); VERITAS, Acciari et al. 2010, data with error-bars) and radio-bands (Baars 1977, circles), as well as the power-law approximation of Suzaku X-ray data (Maeda et al. 2009, diamonds) from the whole remnant are also shown.

W28 profiles at T=37 kyrs

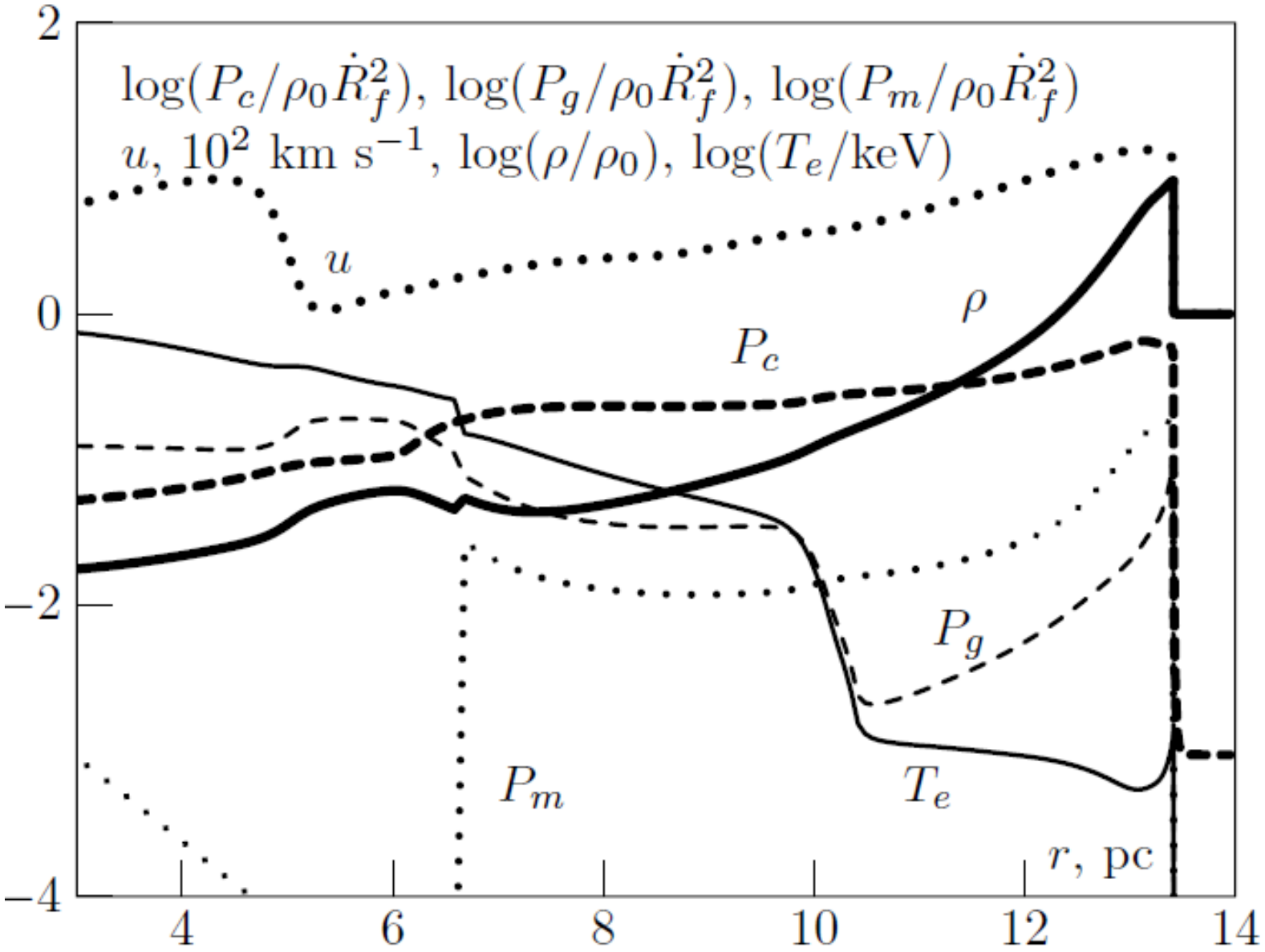

Spectra of particles at T=37 kyrs

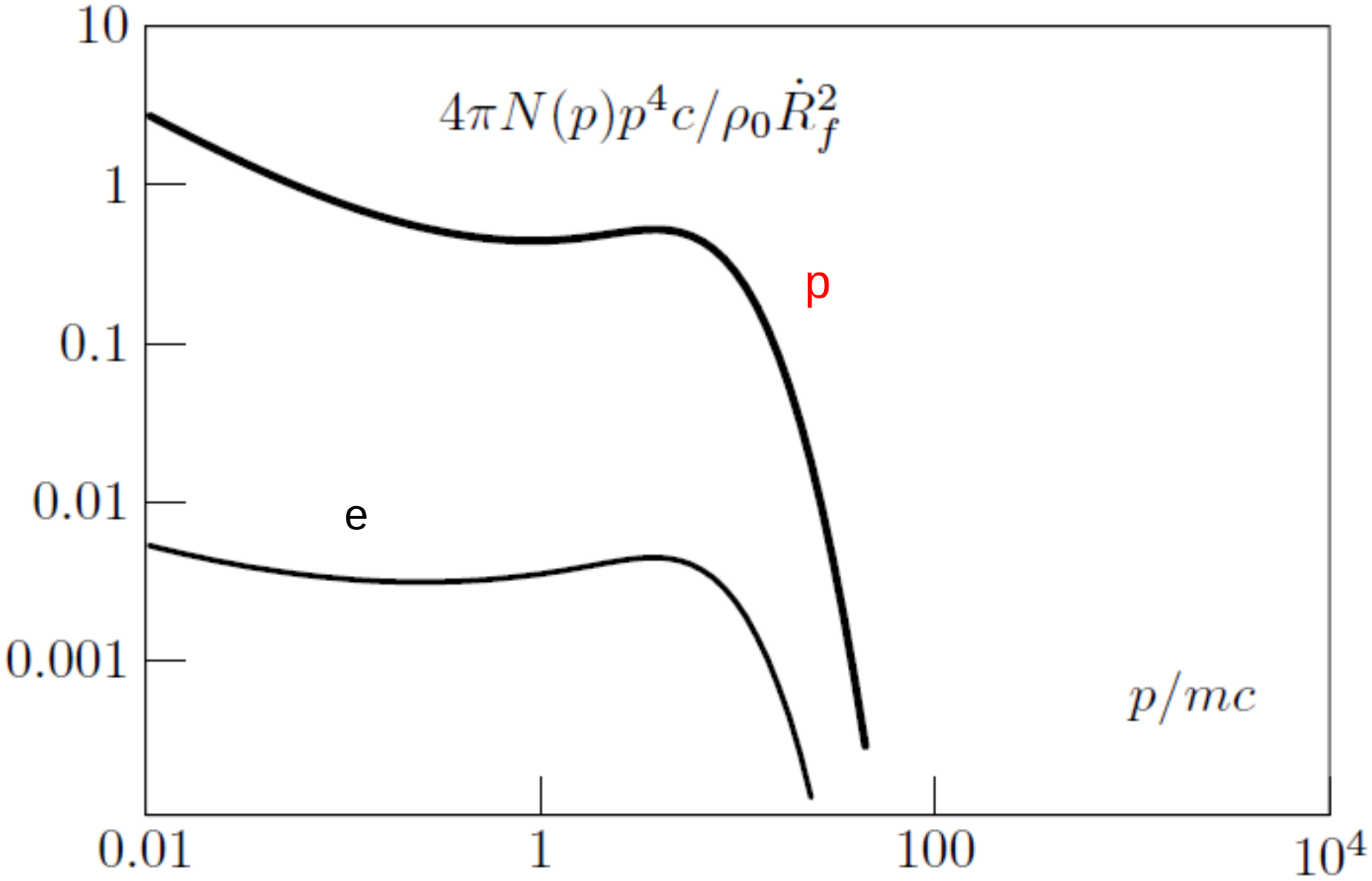

Spectra of particles produced in W28

80 % of energy is transferred to CRs

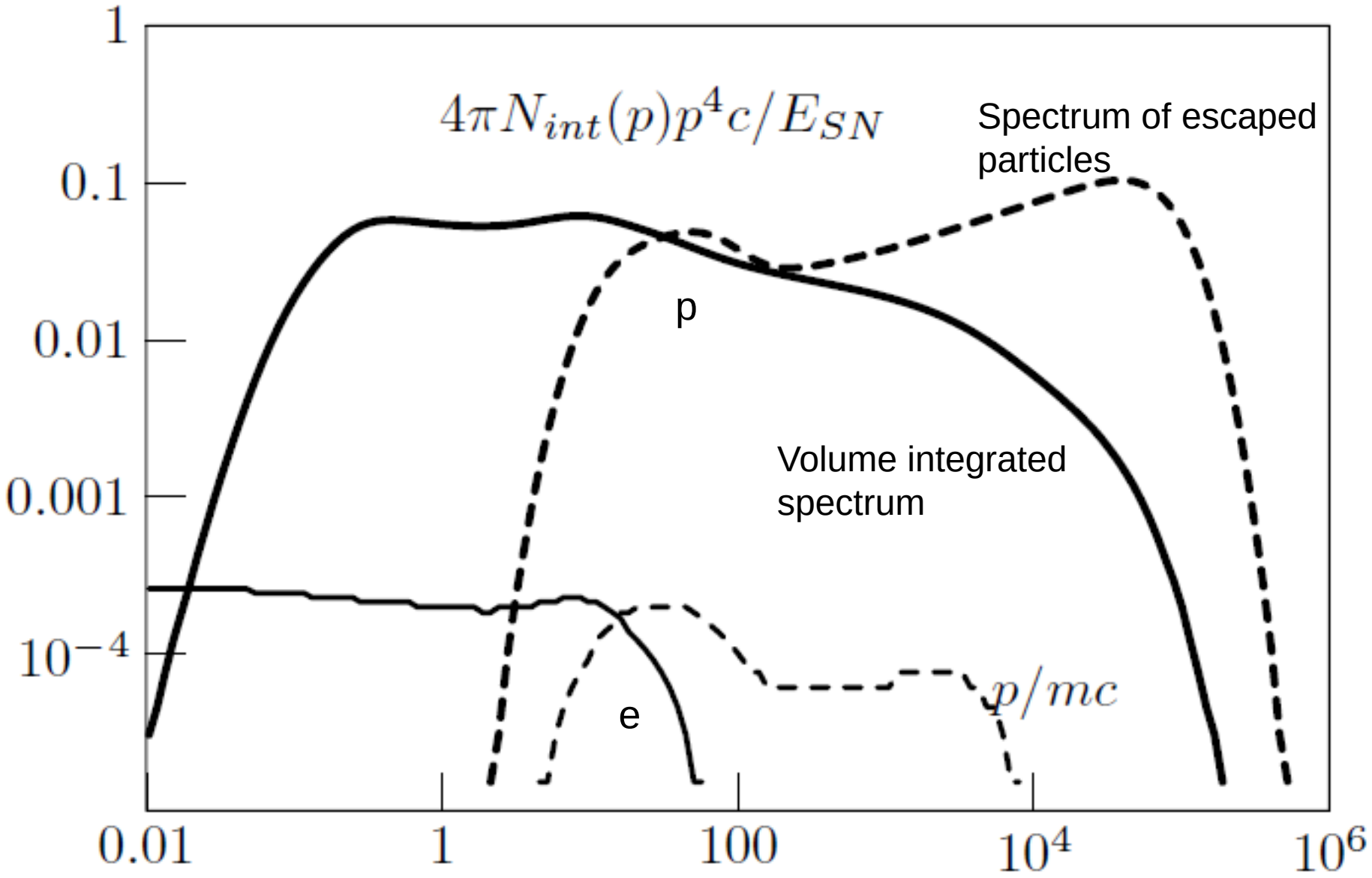

Spectra of W28

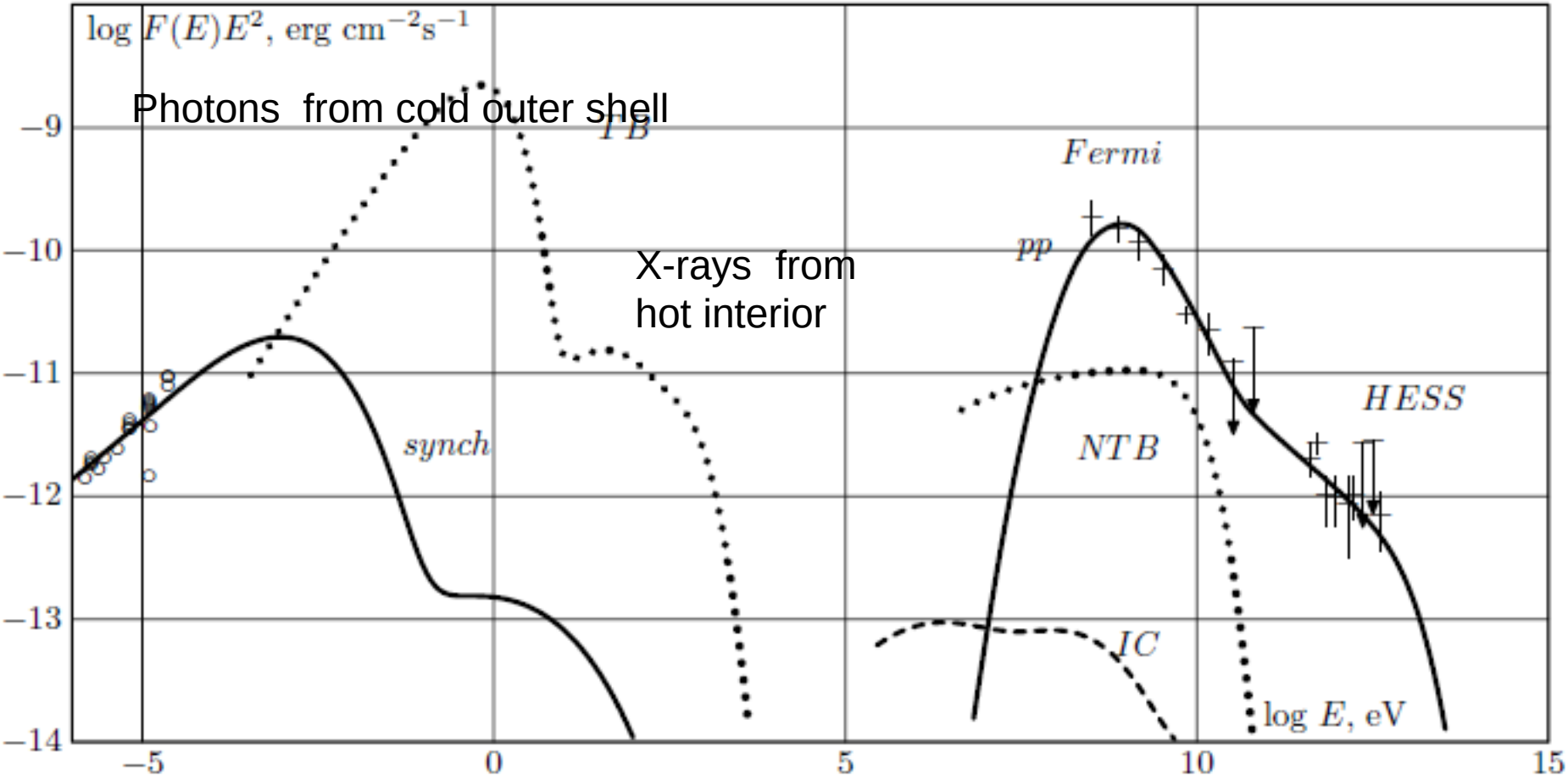

d=1.9 kpc, E_{SN}=1.3·10^{51} erg, M_{ej}=6.8 M_{sol}, t=37 kyr, n_H=4.0 cm^{-3}, n_n=0.2 cm^{-3}

V_f=120 km/s, B_f=8 10^{-5} G, K_{ep}=0.008

Is the number of such SNRs enough for origin of galactic CRs?

YES

$L_{SNR} \sim E_{SN}/T \sim 10^{39}$ erg/s

$L_{SNR} \sim E_{SN}/T \sim 10^{41}$ erg/s for Cas A

100 such SNRs can provide Galactic CR power

Fermi LAT detected about 20 brightest and closest SNRs of this kind with gamma ray energy flux
$F>10^{-11}$ erg cm^{-2} s^{-1}

But modest maximum energies close to 100 TeV

“Knee” energies for SNRs in different circumstellar media (Bohm diffusion in the amplified magnetic field - optimistic estimate)

Uniform medium

SNRs of Ia, IIP supernovae

$$E_{\rm knee} = 3Z\ {\rm PeV}\left(\frac{E_{SN}}{10^{51}{\rm erg}}\right)\left(\frac{M_{ej}}{M_{\rm solar}}\right)^{-2/3} n_H^{1/6}$$

Stellar wind

$$E_{\rm knee} = 80Z\ {\rm PeV}\left(\frac{E_{SN}}{10^{52}{\rm erg}}\right)\left(\frac{M_{ej}}{10M_{\rm solar}}\right)^{-1}\left(\frac{\dot{M}}{10^{-2}M_{\rm solar}{\rm yr}^{-1}}\right)^{1/2}\left(\frac{u_w}{100\ {\rm km/s}}\right)^{-1/2}$$

SNRs of IIP, IIb, IIn supernovae

quasi-parallel shocks, nonresonant instability (Bell 2004)

10 (75 for non linear regime) times lower energies

higher for oblique shocks

Young SNRs with maximal magnetic amplification

Cas A T=350 yr

n_H ~ 0.3-1 cm^{-3}

Tycho T=444 yr

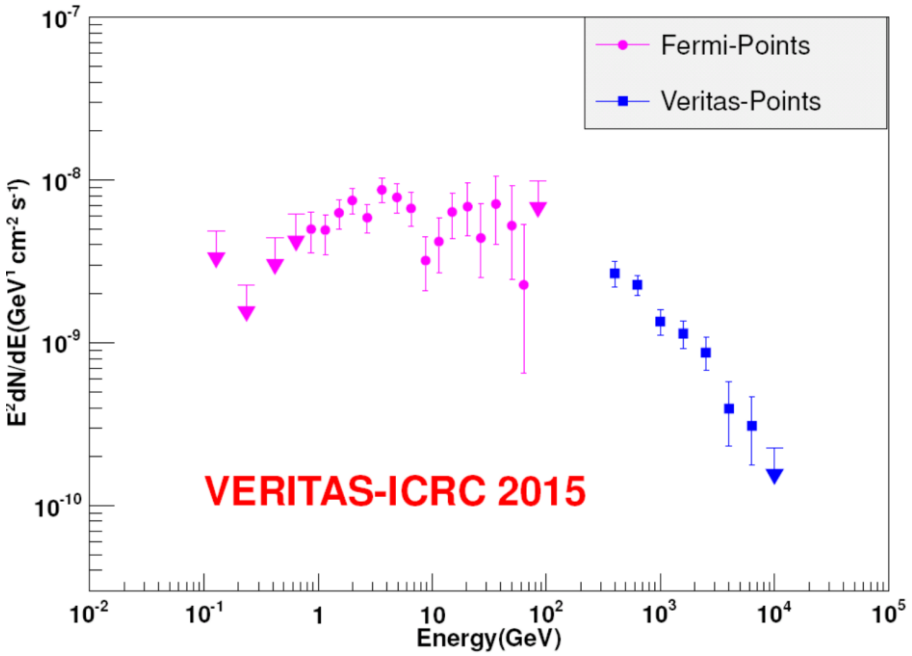

Kumar 2015

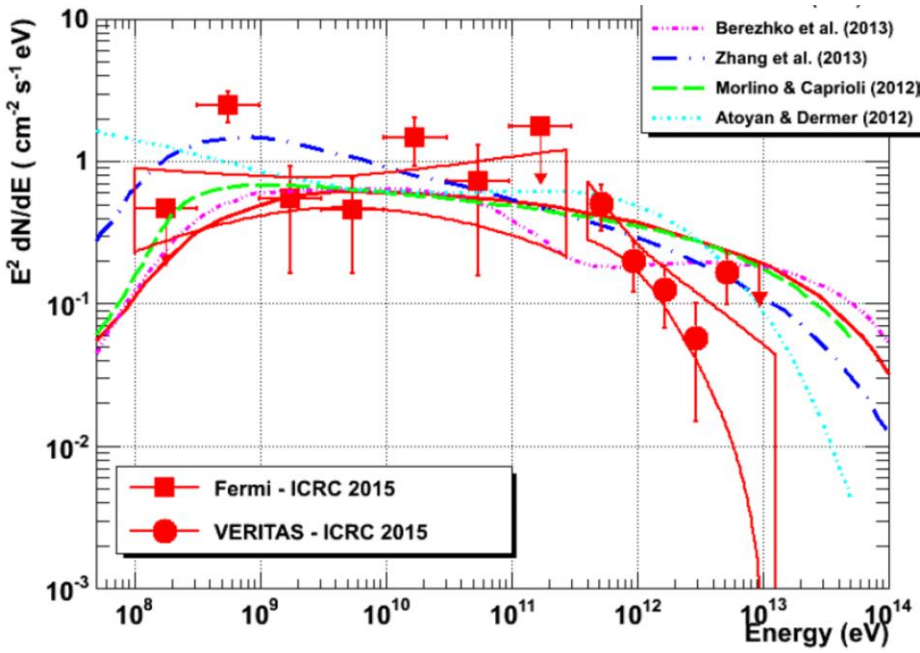

Park 2015

Hadronic origin of gamma-emission, spectral breaks at E_b ~ 300 GeV are observed. The bad accelerators at multi-TeV energies of protons.

Young SNRs in low density medium – in bubbles produced by stellar winds of SN progenitors

RX J1713.7-3946

$n_H \leq 0.1 cm^{-3}$

RCW86

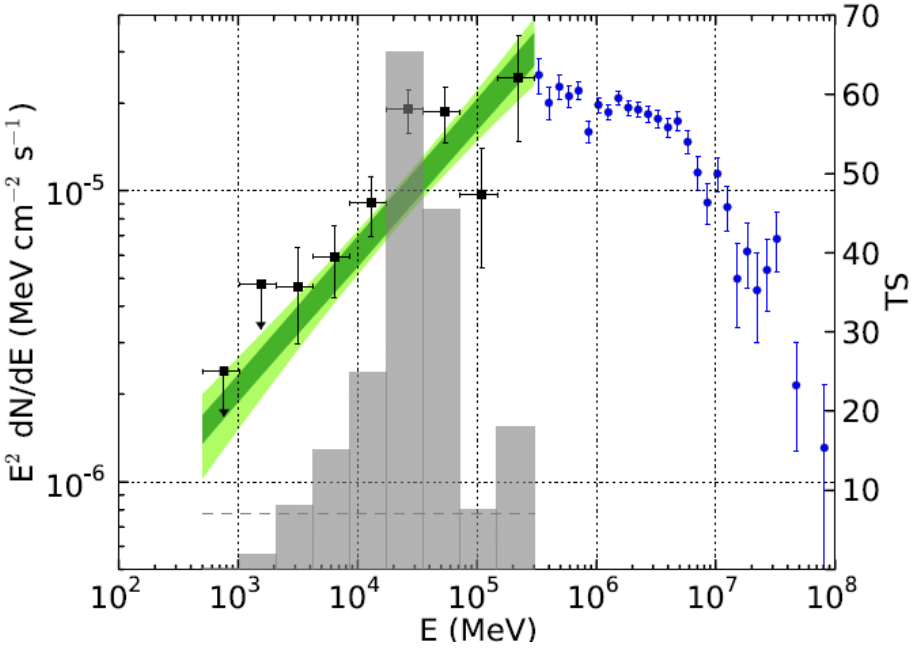

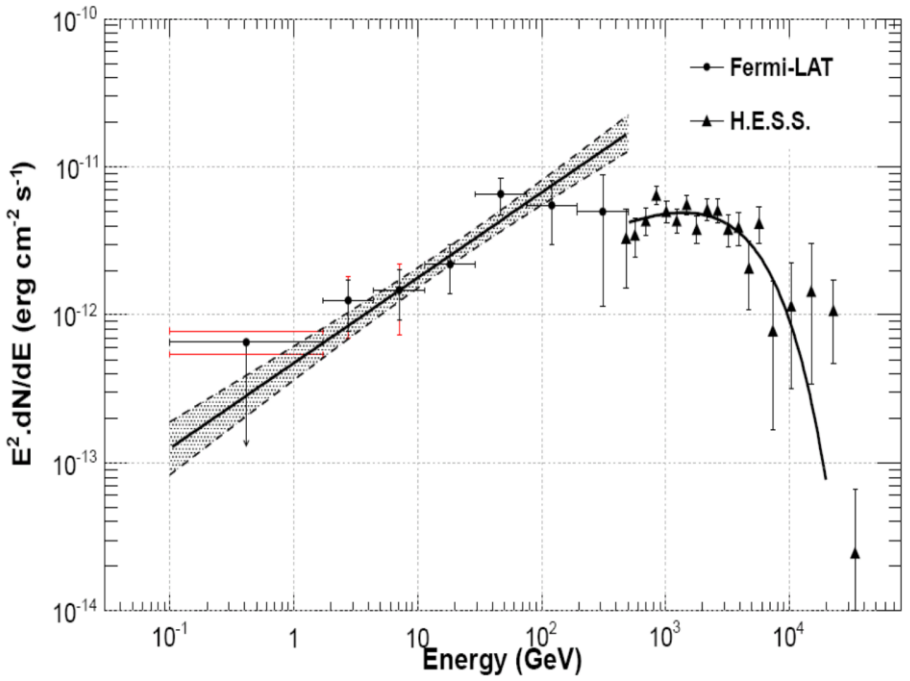

Federici et al. 2015

T~1600 yr

Ajello et al. 2016

T~2000 yr

Probably the leptonic origin of gamma emission, however hadronic gamma rays from strongly modified shock are not excluded. In both cases protons are accelerated up to energies ≥100 TeV.

DSA in wind blown bubbles (Zirakashvili, Ptuskin 2018)

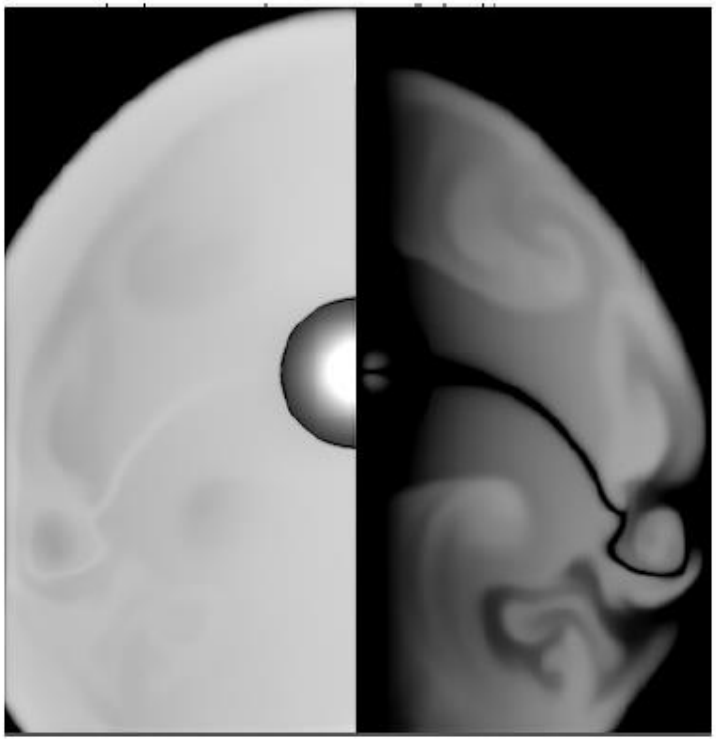

Figure 1: Gas pressure P_g (left panel) and magnetic ter
(right panel) distribution in the domain 10×20 pc at t :
The logarithmic scaling is from $2.3 \cdot 10^{-12}$ erg cm^{-3} (bl
$2.3 \cdot 10^{-10}$ erg cm^{-3} (white color).

$$\dot{M} = 10^{-5} M_\odot \mathrm{yr}^{-1}$$

u_w=1000 km/s, M_w=20, t=300 ky
n_0=10 cm^{-3}

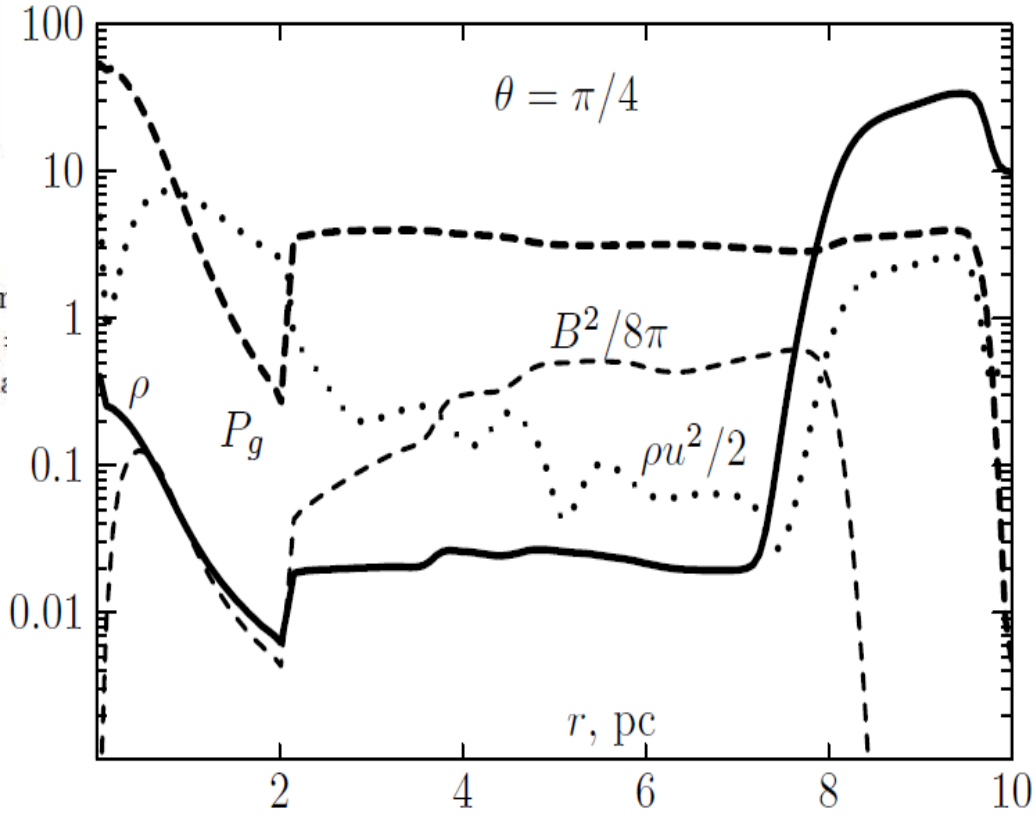

The proper stellar motion 10 km/s was taken into account

B ~ 20 μG at the periphery

DSA in stellar winds

Suggested by Völk & Biermann 1988
DSA at quasiperpendicular shock, faster acceleration
(Jokipii 1986, Takamoto & Kirk 2015)
But problems with injection of ions

$$D_B(E_{\max}) = \kappa V_s R_s \quad \kappa \sim 0.03 - 0.3$$

$$E^w_{\max} = 3\kappa q B V_s R_s / c = \frac{3\kappa}{M_w}\frac{qV_s}{c}\sqrt{u_w \dot{M}} =$$

$$70\, Z\ \mathrm{PeV}\,\frac{3\kappa}{M_w}\frac{V_s}{c}\left(\frac{\dot{M}}{10^{-5} M_\odot \mathrm{yr}^{-1}}\right)^{1/2}\left(\frac{u_w}{10^3\ \mathrm{km\ s}^{-1}}\right)^{1/2}$$

E_{max} =35 TeV for Ib/c SNR: V_s=10^4 km/s,
M_w=20, κ=0.1

Acceleration at TS of the solar wind

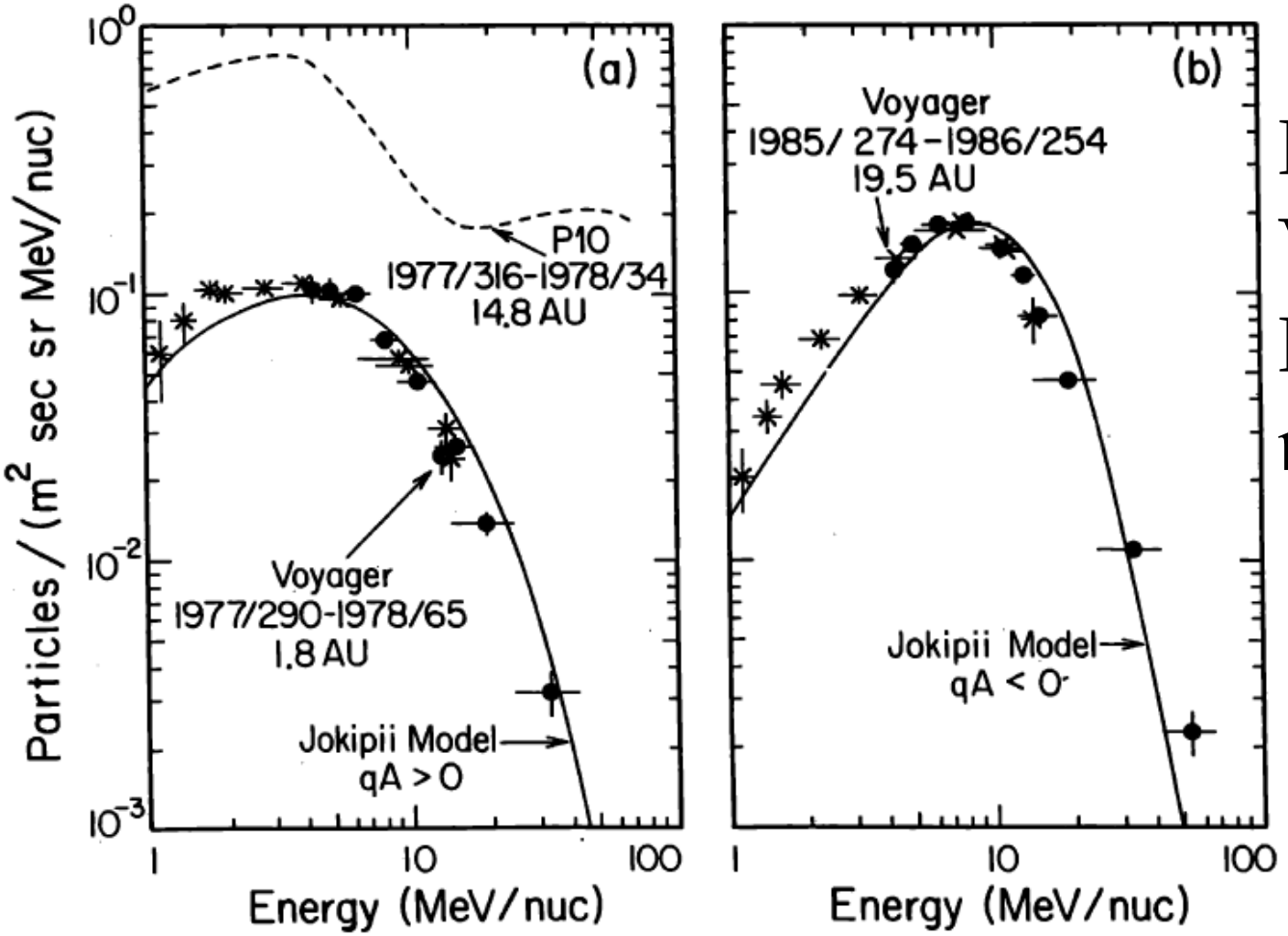

E_{max} =150 MeV
V_s=400 km/s,
M_w=20,
κ=1/3

Cummings, Stone 1987

Fig. 1. (a) Composite ACR energy spectra from Voyager (●, ×) and Pioneer 10 (dashed line) representative of ACR oxygen, as described in the text, for the solar minimum period in 1977-78. The solid line is from the model of Jokipii [6] for the solar magnetic field polarity configuration denoted by "qA>0". (b) Voyager 2 ACR composite energy spectrum for the 1985-86 period. The solid line is from Jokipii for qA<0

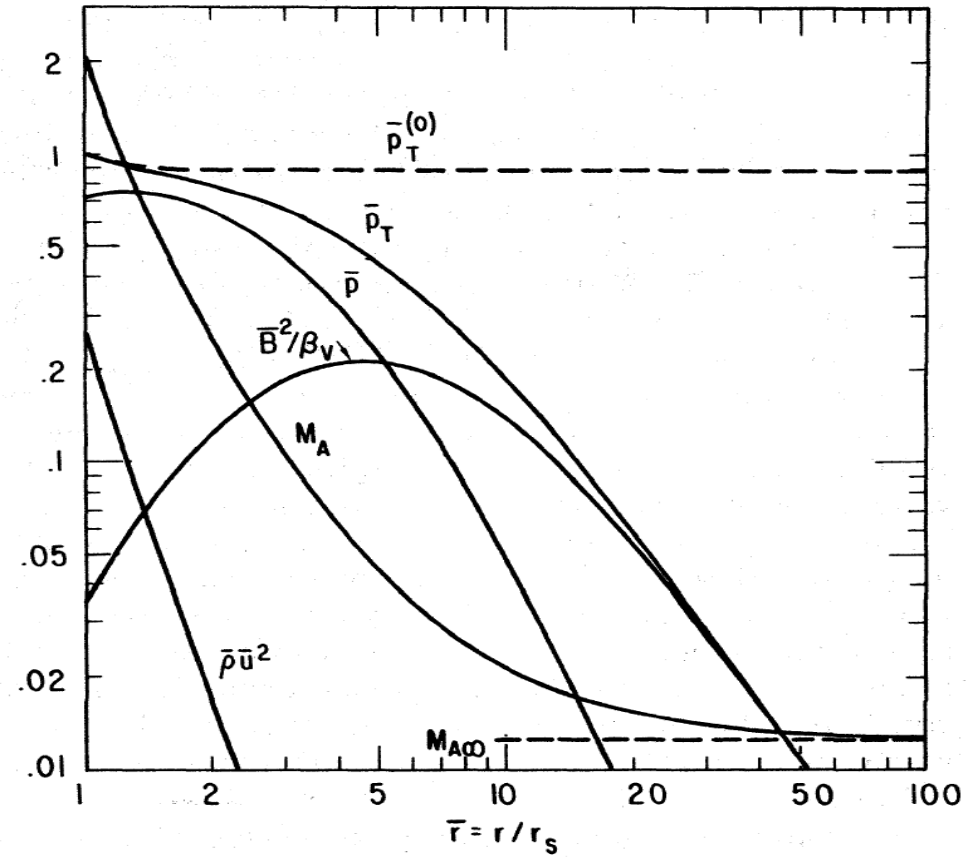

Figure 8 *Solution of equations (34)-(37) with initial conditions determined by equations (30)-(33) and with $\beta_v = 500$. Note that the presence of the magnetic field has caused the total pressure $\bar{p}_T$ to decrease to zero as $\bar{r} \to \infty$, rather than remaining constant ($\bar{p}_T^{(o)}$) as it does in the field-free case* [*from Cranfill, 1971*] .

Amplification of magnetic field downstream of TS (Cranfill 1971, Axford 1972, Chevalier 1992)

Important effect for DSA in the bubbles

$$E^b_{\max} = E^w_{\max} \min\left(\frac{M_w^2}{2}, \sigma_{TS}\frac{R_s^2}{R_{TS}^2}\right)$$

E_{max}=2 Z PeV for Ib/c SNR

Summary

1. Non-resonant streaming instability produced by the electric current of run-away CR particles results in the significant magnetic amplification at fast SNR shocks.

2. Number of observed in gamma rays SNRs have enough CR energy power to explain the origin of galactic CRs. But modest maximum energies ~100 TeV for remnants of IIP SNe.

3. Bubbles produced by O-stars and WR stars are the ideal places for DSA. The magnetic field is amplified by Cranfill effect.

a) Maximum energies > PeV for Ib/c SNRs., slightly below PeV for IIP SNRs. Helium CR composition at Pev energies (WR bubbles)

b) We expect to find several Galactic Pevatrons. With 1000 year age.

c) Expected fluxes of hadronic gamma rays $10^{-12} n^{0.6} d^{-2}_{kpc}$ erg cm^{-2} s^{-1}.